ACS APPLIED MATERIALS & INTERFACES

Research Article

www.acsami.org

Photo-cross-linked and pH-Sensitive Biodegradable Micelles for Doxorubicin Delivery

Jun Chen,[†,‡,§,∥] Jun Ouyang,[#,∥] Jiming Kong,[#,△] Wen Zhong,[*,¶] and Malcolm Mq Xing[*,†,‡,‡,#]

[†]Department of Mechanical and Manufacturing Engineering, [‡]Department of Biochemistry and Medical Genetics, [△]Department of Human Anatomy and Cell Sciences, Faculty of Medicine, [¶]Department of Textile Sciences, Faculty of Human Ecology, University of Manitoba, Winnipeg, Manitoba R3T 2N2, Canada

[‡]Manitoba Institute of Child Health, Winnipeg, Manitoba R3E 3P4, Canada

[#]School of Basic Medical Science, Southern Medical University, Guangdong Provincial Tissue Construction and Inspection Key Laboratory, Guangzhou, China 510515

[§]Key Laboratory for Biomedical Effects of Nanomaterials & Nanosafety, Institute of High Energy Physics, Chinese Academy of Sciences, Beijing 100049, China

Supporting Information

ABSTRACT: Cross-linked polymeric micelles have gained increasing research interest in the past decade due to the instability of existing polymeric micelles when used in vivo. In this study, we reported a series of covalently cross-linked pH-sensitive biodegradable micelles based on the poly(ethylene glycol)-hyperbranched poly(β-aminoester)s with acrylate group terminals (PEG-HBPAE-A) copolymers for intracellular delivery of doxorubicin (DOX). PEG-HBPAE-A can be self-assembled to form micellar nanoparticles in aqueous solution with diameters of approximately 160 nm. The non-cross-linked micelles (NCLMs) were cross-linked upon UV irradiation to form cross-linked micelles (CLMs). ^{1}H NMR, FT-IR and dynamic light scattering (DLS) were utilized to investigate the process of the UV cross-linking and the stability of CLMs. The results showed the significantly enhanced stability for CLMs in comparison to NCLMs. pH sensitivity of CLMs and NCLMs were also estimated by DLS. In vitro drug release studies confirmed that DOX release from DOX-loaded CLMs was greatly inhibited upon the neutral pH environment, whereas DOX underwent faster release in acidic conditions. MTT assays showed that DOX-loaded micelles had a similar inhibition rate for HepG-2 and MCF-7 cell lines compared with free DOX, whereas the blank CLMs and NCLMs showed very low cytotoxicity. Laser scanning confocal microscopy and real-time in situ fluorescence microscopy were exploited to investigate drug uptake in cells and drug distribution in the interior of cells. These results showed a promising nanocarrier for intracellular DOX delivery with great potential for cancer therapy.

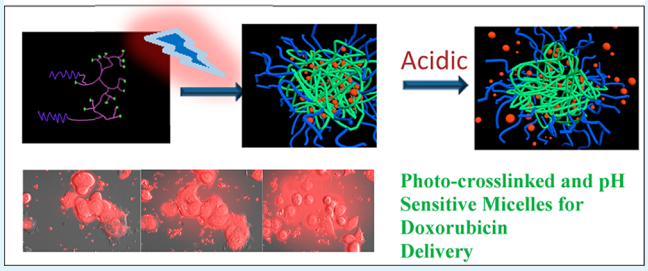

KEYWORDS: *cross-linked micelles, pH sensitive, intracellular drug delivery, poly(ethylene glycol)-hyperbranched poly(β-aminoester)s, doxorubicin, real-time in situ fluorescence microscopy*

INTRODUCTION

Doxorubicin (DOX) has been widely used in the treatment of different types of tumors. DOX can intercalate double strands of DNA to inhibit the biosynthesis of biomacromolecules, so that it is crucial to deliver DOX into the cytoplasm and/or the cell nucleus.[1−6] However, severe and dose-limiting side-effects such as hypersensitivity and cardiotoxicity of DOX seriously impede its clinical application.[5,7] Therefore, it is necessary to develop a safer and more effective DOX delivery system.

Polymeric micelles have been widely researched as one of the most promising nanocarriers for water-insoluble anticancer drugs.[8−10] Normally core−shell micellar structure was achieved from self-assembly of amphiphilic copolymers in aqueous solutions. Those well-developed micellar nanoparticles exhibit a prolonged circulation time by avoiding rapid clearance by the renal and reticuloendothelial systems (RES) due to the small size of the particles and the perfect hydrophilicity and hydratability of the corona consisting of poly(ethylene glycol) (PEG) or dextran.[1,2,11] Stimuli-responsive nanocarriers have been developed to release drugs into tumor tissues upon changes in physical and chemical environments, such as redox potential, pH, temperature, and ultrasound. pH change and redox potential are major chemical stimuli to trigger drug release from cargos.[12−17]

A variety of amphiphilic copolymers can be chosen to build the core−shell architecture of the polymeric micelles. Recently, nanoparticles constituted by poly(β-amino ester)s have been extensively explored as intracellular delivery nanocarrier for

Received: January 2, 2013
Accepted: March 26, 2013
Published: March 26, 2013

anticancer drugs or therapeutic genes.[18−22] The advantages, such as good biodegradability, ease of preparation and controllable functionality, make poly(β-amino ester)s a type of promising polymers in biomedical applications. Moreover, the cationic nature of these polymers endows the derived nanoparticles (polyplexes, micelles, or nanogels) with good cell uptake efficacy and high buffer-capacity to facilitate the nanoparticles escape from endolysomes.[15,17,23] Poly(β-amino ester) consisting of tertiary amines in the backbone has a weakly basic character because of its tertiary amines with a pKb value about 6.5, which renders the polymer water-soluble below pH 6.5 but insoluble at the neutral pH. In our past research,[15] we synthesized poly(β-amino ester)-g-PEG (PAE-g-PEG) graft copolymers constituting tertiary amines and disulfide bonds in backbones, and the copolymers were self-assembled to form pH and reduction dual-responsive micelles. DOX entrapped in these micelles was found to be released at a higher rate at pH 6.5 and/or 5 mM DTT concentration, in agreement with their fast demicellization behavior in a weakly acidic environment and/or stronger reduction environment. In the work of other groups, Shen et al.[24] reported the synthesis of a BAE-PEG, which formed micelles with a core soluble at about pH 6 and a stable PEG corona. These micelles have a lower dissociation pH of 6.1, which was demonstrated to be more suitable for use as a cytoplasmic drug delivery system. Reports showed the high sensitivity of poly(β-amino ester) consisting of tertiary amines in response to a weakly acidic environment and revealed that the hydrophobicity of poly(β-amino ester)s can be tuned to form nanoparticles for both extracellular and intracellular drug delivery.

However, inadequate stability of drug-laden micellar nanoparticles is one major practical challenge in vivo.[25,26] In the past decade, many research groups have developed various cross-linking approaches to enhance micelles stability.[27−29] It is worth noting, nevertheless, that there are only a few reports on the development of cross-linked biodegradable micelles for anticancer drug delivery. For example, Kissel et al.[29] reported that core cross-linked PEG-PCL micelles exhibited significantly enhanced PTX-loading efficiency and thermodynamic stability when diluted. Hennink et al.[30] reported that core cross-linked micelles from PEG-b-p(HPMAm-Lacn) had prolonged circulation time and much higher accumulation in the tumor than those noncross-linked micelles (NCLMs); acid-labile DOX-conjugated core cross-linked micelles resulted in better antitumor activity in B16F10-bearing mice than free DOX. All these designs of copolymer for preparing cross-linked micelles commonly need multiple and complicated synthetic pathways and harsh reaction conditions, which impede the applications of these nanomedicine designs.

In the present work, stable pH-responsive micellar nanoparticles were prepared by photopolymerization of acrylate groups in the hyperbranched poly(β-amino ester)s cores upon UV-irradiation at λ = 254 nm (Scheme 1A, B). The synthetic routine includes two simple steps. First, the hyperbranched poly(β-amino ester)s were synthesized via Michael addition polymerization of 4-(aminomethyl)piperidine (AMP) and excess amount of 1,6-hexanediol diacrylate (HDDA) at 60 °C. Another Michael addition reaction was then allowed to take place between the PEG-NH_2 and the residual acrylate groups in the formed hyperbranched polymer at room temperature to obtain the amphiphilic copolymer denoted PEG-HBPAE-A. These copolymers could self-assemble into micelles in aqueous solution at pH 7.4 spontaneously, with PEG shells and HBPAE

Scheme 1. (A) Formation of Micelles and Crosslinked Micelles with Doxorubicin, And the Size Change of the CLMs Exposed to the Acidic Environment; colors of the Polymer Chains Are in Accordance to Those Shown in the Chemical Structure; (B) Synthesis Routine of Biodegradable Acrylate Terminal Hyperbranched Poly(β-amino ester)s-*b*-poly(ethylene glycol) Amphiphilic Copolymers[a]

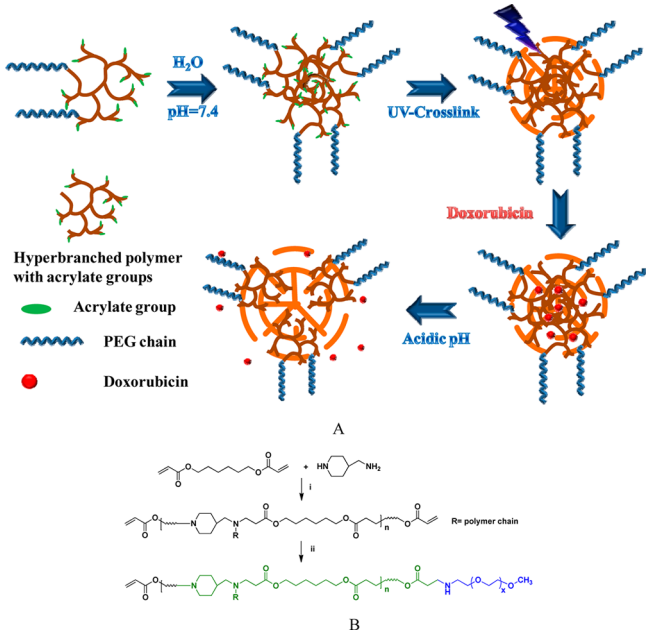

[a]Conditions: (i) chloroform, 60 °C, 3 days; (ii) PEG-amine, room temperature, 3 days.

cores. Cross-linked micelles (CLMs) were prepared through core cross-linking of the micelles under UV-irradiation at λ = 254 nm, and subsequently their stability, pH sensitivity, and DOX release behaviors with different compositions of block copolymers and various solution pH values were investigated. The results indicated that these CLMs have enhanced stability with inhibited release of DOX upon dilution, sharp pH sensitivity, and enhanced in vitro antitumor efficacy.

MATERIALS AND METHODS

Materials. All chemicals were purchased from Sigma-Aldrich Canada Ltd. (Oakville, Ontario, Canada) and used without further purification unless otherwise noted. Methoxy PEG (5K) and Methoxy PEG-NH_2 (mPEG-NH_2) were purchased from JenKem Technology USA Inc. (Allen, TX, US). The 3-(4, 5-dimethyl thiazolyl-2)-2, 5-diphenyl tetrazolium bromide (MTT) cell proliferation assay kits were obtained from Biotium Inc. (Hayward, CA). Dialysis membrane (7 kDa MWCO), 0.45 μm Millipore Millex syringe filters were purchased from Fisher Scientific (Ottawa, ON, Canada). Carbon-coated copper grids were purchased from Canemco Inc. (Core, Quebec, Canada). Human hepatocellular carcinoma cell line (HepG2) was purchased from ATCC. Human breast cancer cell line (MCF-7) was kindly gifted from Dr. A Raouf (Manitoba Cancer Care).

Characterizations. ^{1}H NMR spectra were recorded on a Bruker Avance 300 NMR spectrometer (300 MHz) with $CDCl_3$ as the solvent. The UV absorbance was recorded with a Varian Cary-50 UV−vis spectrophotometer. The fluorescence intensity of pyrene was recorded with a Varian Cary Eclipse fluorescence spectrophotometer. The number average (Mn), weight average (M_w) molecular weight and polydispersity index (PDI) M_w/M_n were determined by a size exclusion chromatography (SEC) system consisting of Shimadzu LC-10ADVP solvent delivery unit, a CTO-10ASVP Shimadzu column

oven and a Polymer Laboratories PL-gel 5 μm mixed C column. The system was also equipped with a mini DAWN triangle light scattering detector and an OPTILAB DSP interferometric refractometer (both are from Wyatt Technology, Santa Barbara, CA). Tetrahydrofuran (THF)/N,N-Dimethylformamide (DMF) (v/v = 9/1) was used as eluent at a flow rate of 1.0 mL/min and temperature of 30 °C. SEC data were analyzed using Astra software from Wyatt Technology. Refractive index increments (d*n*/d*c*) were determined by an interferometric refractometer and used in the SEC analysis. Images of the micelles were recorded by a Joel 1010 Transmission Electron Microscope (TEM) at 80 KV using a LaB6 filament and recorded using an AMT digital camera. Micrographs were collected at 60 000× magnification. Hydrodynamic diameters (Dh) and size distributions were determined by Malvern Zetasizer Nano-S dynamic light scattering (DLS) (Malvern Instruments Ltd. Worcestershire, UK). Measurements were conducted at room temperature.

Synthesis and Characterization of PEG-HBPAE-A Copolymers. The copolymer PEG-HBPAE-A was typically synthesized as follows: 1,6-hexanediol diacrylate (HDDA, 406.8 mg, 1.8 mmol) and 4-(aminomethyl) piperidine (AMP, 91.2 mg, 0.8 mmol) were added into a 20 mL borosilicate vial, and 5 mL of chloroform was added to dissolve the mixture into a clear solution. The reaction lasted for 3 days at 60 °C to yield poly(β-aminoester)s precursors with residual acrylate as end groups (HBPAE-A). ^{1}H NMR (ppm): δ 1.30−1.50 (-CH2(C*H2*)2CH2-, -(HC*H*)2-CH-), 1.50−1.70 (-C*H2*-CH2-CO-, -(HC*H*)2-C*H*-), 2.20 (CH-C*H2*-N-), 2.30−2.50 (-C*H2*COO−), 2.60−2.90 (-CH2N(C*H2*)2-) 2.90−3.00 (-C*H2*NHC*H2*-), 4.0−4.2 (-COOC*H2*-), 5.8−6.4 (C*H2*═C*H*-CO-).

PEG5K-NH_2 (600 mg, 0.12 mmol) was then added. The reaction was performed at room temperature for 3 days. The mixture was precipitated in a large excess amount of cold diethyl ether, and finally dried in vacuum. The final product was stored at −20 °C and kept dark. The typical yielding of the copolymer was about 60%. ^{1}H NMR (ppm): δ 1.30−1.50 (-CH2(C*H2*)2CH2-, -(HC*H*)2-CH-), 1.50−1.70 (-C*H2*-CH2-CO-, -(HC*H*)2-C*H*-), 2.20 (CH-C*H2*-N-), 2.30−2.50 (-C*H2*COO-), 2.60−2.90 (-CH2N(C*H2*)2-) 2.90−3.00 (-C*H2*NHC*H2*-), 3.50−3.7 (-C*H2*OC*H2*-), 4.0−4.2 (-COOC*H2*-), 5.8−6.4 (C*H2*═C*H*-CO-).

Formation of Micelles and Critical Micelle Concentration Determination. The PEG-HBPAE-A micelles were prepared using the dialysis method. PEG-HBPAE-A copolymer (20 mg) was dissolved in 2 mL of DMF while being stirred. Ten ml of phosphate buffer (PB, pH 7.4, 10 mM) was added dropwise with constant stirring. The solution was then dialyzed against PB (pH 7.4, 10 mM) for 24 h (molecular weight cutoff = 7000) to form the micelles.

The critical micellation concentration (CMC) of PEG-HBPAE-A copolymer in water was estimated by fluorescence spectroscopy using pyrene as a probe. Twenty microliters of pyrene acetone solution (20 μg/mL) were added to 4 mL vials, and then acetone was allowed to evaporate to dry. Four milliliters of an aqueous solution containing 0.1−128 mg/L PEG-HBPAE copolymers were added to the vials. Therefore, the final concentration of pyrene in each sample solution was 0.1 μg/mL. The excitation spectra (300−360 nm) of the solutions were recorded when the emission wavelength was set at 395 nm and the slits were adjusted to give a bandwidth of 5 nm for the excitation and emission beam recorded as emission wavelength of 395 nm with the excitation and emission bandwidths set at 5 nm. The ratios of the peak intensities at 338 nm over 334 nm (I338/I334) of the excitation spectra were recorded and plotted versus polymer concentration. The CMC value was taken from the intersection points of the tangent to the curve at the high concentrations with the horizontal line through the point at the low concentrations.

Hydrodynamic diameter and size distribution of the micelles were determined by dynamic light scattering (DLS). Measurements were carried out at 20 °C using Zetasizer Nano-S from Malvern Instruments. Solution of the micelles was passed through a 0.45 μm pore size syringe filter prior to being measured. The morphology of micelles was examined by transmission electron microscopy (TEM). The digital images were recorded by a Joel 1010 TEM at 60 KV using a LaB6 filament and recorded using an AMT digital camera. The TEM samples were prepared as below: a drop of the isolated micelle solution was drop-cast on a carbon coated copper grid (400-mesh) and dried by filter paper. Then 2% (w/v) of uranyl acetate solution was dropped on the grid. One minute of contact was allowed before excess liquid was removed using filter paper. The grid was air-dried for 1 h before being observed under a microscope. Then average diameter of particles was then measured from 10 particles in the TEM micrographs.

UV Cross-Linking of PEG-HBPAE-A Micelles. The UV initiator, 2,2′-azobis(2-methylpropionitrile) (AIBN), which has been widely used to prepare photocross-linked hydrogels was employed as a photoinitiator to cross-link the micelles. Acetone solution of AIBN (25 μL, 10 mg/mL) was introduced into a micellular solution of PEG-HBPAE-A (1 mL, 1 mg/mL), resulting in a final AIBN concentration of 0.05 wt %. The mixture was ultrasonicated for 1 h to evaporate acetone. Then, the micellular solution was irradiated under the UV light (XL-1000 UV-cross-linker, Spectronics) with 40 mW/cm^2 for 1 h to yield CLMs. The CLMs and the corresponding NCLMs were studied in terms of size and stability against extensive dilution by phosphate buffer saline (PBS) buffer and medium supplement with 10% FBS and 1% P/S.

Preparation of DOX-Loaded PEG-HBPAE Copolymer Micelles. DOX-loaded micelles of PEG-HBPAE-A copolymers were prepared as follows: briefly, DOX (1 mg) dissolved in 1 mL of DMF was stirred with 1.5 equiv. of triethylamine, followed by addition of 20 mg of CLMs and stirring for another 30 min. Five milliliters of distilled water was added dropwise under vigorous stirring. The dispersed DOX-loaded polymeric micelles were dialyzed for 24 h (molecular weight cutoff = 7000) to remove free DOX and byproducts. Finally, the DOX-loaded micelles were lyophilized to give a red powder. By using UV−vis spectroscopy, the drug-loading efficiency of DOX-loaded polymeric micelles dissolved in DMF was quantified by referring to its absorbance at 480 nm. For determination of drug-loading content, DOX-loaded micelles were dissolved in DMF and analyzed with fluorescence spectroscopy, wherein a calibration curve was obtained with DOX/DMF solutions of different DOX concentrations.

Drug-loading content and drug-loading efficiency were calculated according to the following equations:

$$\text{drug-loading content as a percentage} = (\text{weight of loaded drug}/(\text{weight of copolymer} + \text{weight of loaded drug})) \times 100\%$$

$$\text{drug-loading efficiency as a percentage} = (\text{weight of loaded drug}/\text{weight of feeding drug}) \times 100\%$$

In Vitro DOX Release from Copolymeric Micelles. The pH-dependent DOX release measurements were carried out as below: dispersed DOX-loaded polymeric micelles were added to a dialysis membrane tube (molecular weight cutoff = 7000), which was then incubated in 30 mL of acetate buffer at pH 5.0 or PBS at pH 7.4 at 37 °C in a water bath with a shaking rate of 80 rpm. At predetermined frequencies, 6 mL of incubated solution was taken out and 6 mL of fresh buffer was added to refill the incubation solution to 30 mL. pH-dependent DOX release profiles were determined by measuring the UV−vis absorbance of the solutions at 480 nm.

Cytotoxicity of DOX-Loaded CLM and NCLM Micelles. MCF-7 cell line was used to investigate cell inhibition of DOX-loaded micellar nanoparticles. MCF-7 cells were cultured with Dulbecco's Modified Eagle's Medium (DMEM, GIBCO) supplemented with 10% fetal bovine serum (FBS, GIBCO), 1.0 × 10^5 U/l penicillin (Sigma) and 100 mg/L streptomycin (Sigma) at 37 °C in 5% CO_2.

The cytotoxicity of the copolymeric micelles loaded with DOX was determined using a MTT cell proliferation kit (Biotium Inc.). MCF-7 cells were seeded into a 96-well tissue culture plate at a density of 8,000 cells per well and were incubated at 37 °C in 5% CO_2. The growth medium was replaced with fresh DMEM after 24 h. Then the DOX-loaded PAE polymeric micelle solution and controls (free DOX

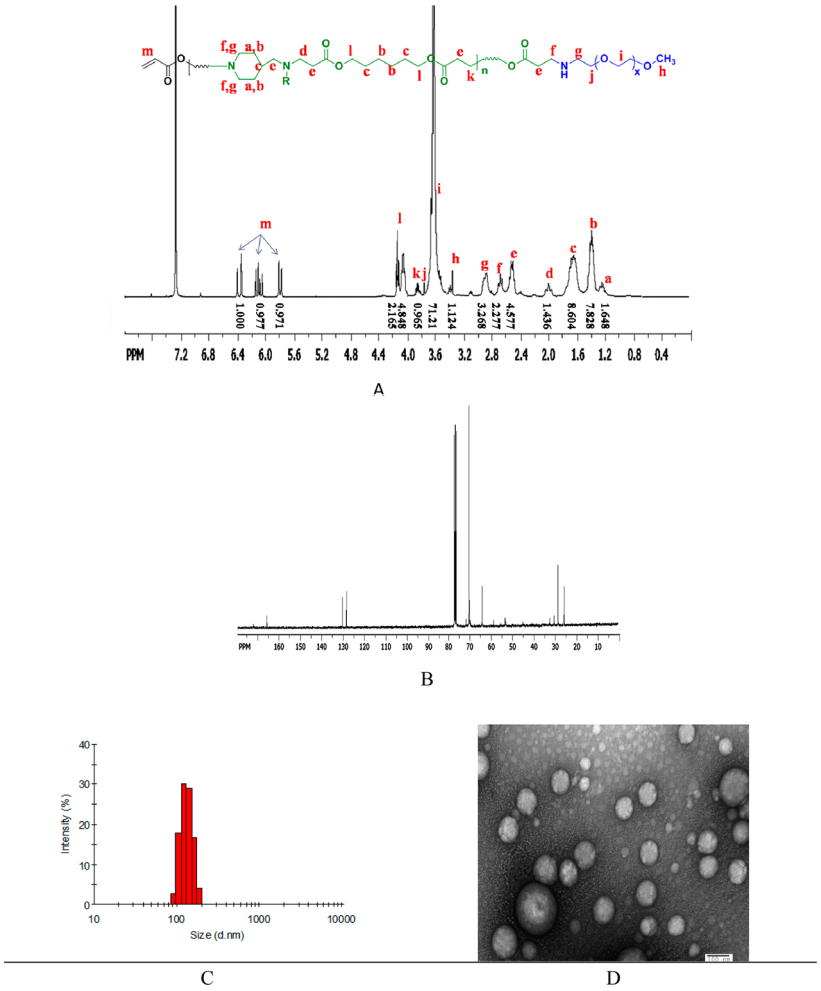

Figure 1. (A) ^{1}H NMR spectrum of PEG5K-HBPAE-A copolymer with integration; (B) ^{13}C NMR spectrum of PEG5K-HBPAE-A copolymer; (C) typical size and size distribution of CLMs determined by DLS; D) Typical TEM micrograph of CLMs. scale bar = 100 nm.

and blank micelle solutions) were added into wells (six wells per sample). After 24 or 48 h of incubation, 10 μL MTT solution was added to each well and incubation continued for another 4 h. The medium was removed and 200 μL DMF was added into each well to dissolve the formazan by pipetting in and out several times. The absorbance of each well was measured using an ELISA plate reader at a test wavelength of 570 nm and a reference wavelength of 630 nm. The cell inhibition of samples was calculated as:

$$\text{cell inhibition}(\%) = \frac{I_{\text{control}} - I_{\text{sample}}}{I_{\text{control}}} \times 100\%$$

Where I_{sample} and I_{control} represent the intensity determined for cells treated with different samples and for control cells (untreated), respectively.

Cellular Uptake of DOX-Loaded CLM and Intracellular Drug Distribution. Confocal laser scanning microscopy (CLSM) was employed to examine the cellular uptake of DOX by incubating the HepG2 cells with free DOX or the DOX-loaded CLM for 15 min, 2 or 24 h. First, the HepG2 cells were seeded in the culture dish with a coverslip at a density of 2 × 10^5 cells/dish (diameter = 3.5 cm) and cultured for 24 h. Then the cells were exposed to DOX-loaded micelles. After a predetermined incubation time, the coverslip was washed with cold PBS three times, and cells were fixed by 4% paraformaldehyde in PBS at room temperature for 15 min. After fixation, the cells were permeabilized by 0.1% Triton X-100 in PBS for 10 min and then rinsed with PBS three times. The cells were incubated in 0.1 μM BODIPY FL phallacidin/1% (w/v) BSA solution for 20 min and then rinsed with PBS three times. The cells then were incubated in 1 μM Topro-3 for 20 min and then rinsed with PBS three times. The coverslip was set on a microscope slide and examined by CLSM.

Real-Time in Situ Imaging of DOX Release from DOX-Loaded CLMs in Living Cells. The cellular uptake and intracellular release behaviors of DOX-loaded CLMs were also evaluated with Olympus Vivaview FL incubator supply with fluorescence microscopy (LCV110U, Olympus Co., Ltd., Tokyo) using MCF-7 cells. The cells were cultured in a disc (diameter = 3.5 cm) containing 2 mL of DMEM media for one day to ~60% confluency (2 × 10^5 cells/disc), 20 μL of PBS (pH 7.4) solution of DOX-loaded CLMs containing 20 μg of DOX was added. The disc were transferred into the Olympus Vivaview FL incubator setting at 37 °C in a 100% humidified 5% CO_2-containing atmosphere. After ~1 h of stabilization, the fluorescence microscope was set to collect differential interference contrast (DIC) images for observation of morphology of MCF-7 cells and fluorescence image from doxorubicin for every 15 min in 24 h. The cells were visualized with a 40× objective lens (UAP040X/340, NA 0.9, Olympus) using standard filter sets and a mercury lamp. Sequential images were acquired with a cooled charge-coupled device camera (DP30BW, Olympus) with a certain exposure time every 15 min. Data were analyzed using Image J 1.46 software from NIH.

RESULTS AND DISCUSSIONS

Synthesis of PEG-HBPAE-A Copolymer. In this study, we devised robust core cross-linked biodegradable micelles for the challenge of future application in vivo. To this end, we adopted a two-step method to synthesize the PEG-HBPAE-A copolymers. First, the hyperbranched poly(β-amino ester)s

were synthesized through feeding excess diacrylate monomer (HDDA) to trifunctional amine 4-(aminomethyl)piperidine (AMP) via Michael addition polymerization, which is extensively used to prepare polymers to derive biodegradable backbones and introduction of functional groups in contrast to radical polymerization. This PAE polymer was exploited to constitute the core of the micelles and the surplus acrylate groups were designed to be second conjugated by mPEG-NH_2 to obtain the amphiphilic copolymers. Afterward, the residual acrylate groups will be used to form the cross-linked core upon UV-irradiation resulting in superior micelles stability.

In the Michael-type addition polymerization, the amine reactivity follows the sequence of 2° amine (on the ring of piperazine or piperidine) > 1° amine ≫ 2° amine (formed), and equal molar ratio of trifunctional amine monomer to bisacrylate monomers produces linear polymer;[31] however, decreased molar ratio of trifunctional amine monomers to bisacrylate monomers tends to produce hyperbranched polymer because the large excess of acrylate groups accelerate consuming the 2° amines to construct a branched architecture. Furthermore, the significant increase of the activity of formed secondary amine in Michael type addition was achieved by elevating the polymerization temperature as shown by Hong et al.[32] They reported that the relative reactivity of the formed secondary amines is significantly enhanced by elevating reaction temperature to above 48 °C, when hyperbranched polymers are formed.

Michael addition polymerizations of amine groups in trifunctional amine monomers (AMP) and acrylate groups in diacrylate monomers (HDDA) at a 1/1.5 molar ratio were carried out in chloroform solution at 60 °C to form poly(*β*-amino ester)s with hyperbranched architecture. After 3 days polymerization, the mixture became viscous. Subsequently, the mPEG-NH_2 was added to further conjugate with the surplus acrylate terminals in the produced hyperbranched polymers (HBPAE-A) at 1/5 molar ratio of amine groups in PEG-NH_2 to acrylate terminals in HBPAE-A. The typical ^{1}H NMR with integrations and ^{13}C NMR spectra are shown in Figure 1. ^{1}H NMR spectrum displayed characteristic signals of PEG (δ 3.60) and PAE (δ 4.20, 3.20, 2.80, 2.40, 1.65, and 1.35) also resonances of acrylate terminal (δ 5.80, 6.20, and 6.40) (Figure 1A). GPC-light scattering revealed that the obtained two copolymers had a unimodal distribution with a polydispersity of around 2.0 and Mn of around 9.0 kg/mol. According to the integrals of the characteristic peaks in ^{1}H NMR spectra and the number average molecular weight, it was found that the ratio of the acrylate terminal groups to PEG chain was ∼15, and each copolymer composed of one PEG chain. This two-stepped reaction underwent simple and widely used synthesis methods,[33] which could be recognized as a new approach to synthesizing the macromonomers based on hyperbranched polymers.

To investigate the reactivity of the acrylate groups in the produced PEG-HBPAE-A copolymer, the acrylate terminal was designed to be readily converted into hydroxyl groups by the addition of 2-mercaptoethanol in the presence of AIBN in DMF at 70 °C according to the method reported in the references.[34−36] As shown in Figure 2A, ^{1}H NMR spectrum showed that peaks attributed to the vinyl protons (δ 5.80−6.45) completely disappeared, while new peaks attributed to 2-mercaptoethanol groups were detected at δ 2.5 and 3.3 (Figure 2A), indicating quantitative conversion of acrylate to hydroxyl groups. After UV irradiation for 60 min, the characteristic IR

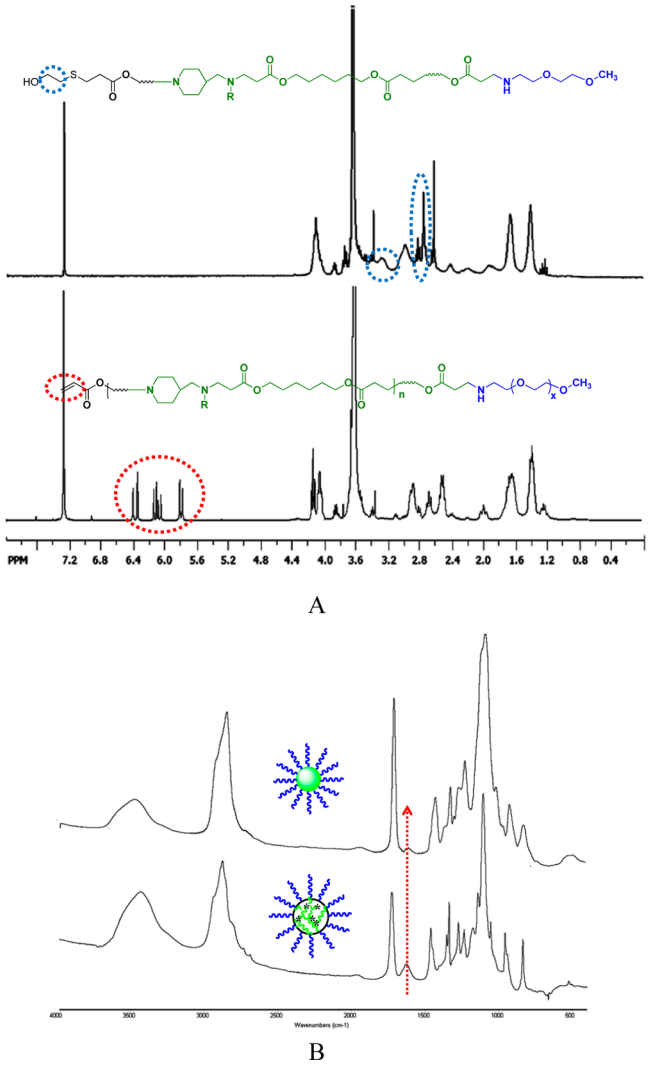

Figure 2. (A) ^{1}H NMR spectrum of PEG-HBPAE-Acrylate in $CDCl_3$ compared with ^{1}H NMR spectrum of PEG-HBPAE-mercaptoethanol. The red circle highlights the disappearance of characteristic peaks attributed to the acrylate groups, and the blue circle hightlights the appearance of the characteristic peaks attributed to the conjugated mercaptoethanol; (B) the FT-IR spectra of NCLMs and CLMs copolymeric micelles in the 500−4000 cm^{-1} region.

absorbance at 1636 cm^{-1} clearly decreased, which attributed to the stretching of double bonds. The ratios of peaks at 1735 cm^{-1} (stretching of C═O in ester groups) to the peaks at 1636 cm^{-1} suggest that there was very small amount of residual double bonds after exposure to the UV irradiation.

The critical micelle concentration (CMC) of the PEG-HBPAE-A copolymer was investigated by fluorescence spectrometry using pyrene as a probe. Pyrene has been widely used as a hydrophobic fluorescence probe for micellar core−shell architecture formation, in which, the ratio I338/I334, defined as the intensity of the first vibration band relative to the third vibration band, can be used as an index of micelle hydrophobicity. The intensity ratio of I338/I334 was used to assess the hydrophobicity of the core. The CMC value was defined as the concentration corresponding to crossing point of the tangent to the curve with the horizontal tangent through the point at the low concentrations. As shown in Table 1, the CMC of PEG5000-HBPAE-A and PEG2000-HBPAE-A copolymer was about 15.0 μg/mL and 20.8 μg/mL, respectively,

dx.doi.org/10.1021/am400017q | ACS Appl. Mater. Interfaces 2013, 5, 3108−3117

Table 1. Characterization of Chemical Composition of the PEG-HBPAE copolymers

samples	M_n (KDa)	M_w (KDa)	PDI	CMC (μg/mL)	micelle diameter (nm) non-cross-linked	micelle diameter (nm) cross-linked
PEG5000-HBPAE-A	9.34	18.59	1.99	15.0	163	140
PEG2000-HBPAE-A	8.16	13.04	2.11	20.8	135	118

in a phosphate buffer (PB, pH 7.4, 10 mM), indicating that a core−shell structure was formed in such a low concentration compared to the existing micelles in previous reports.[37−39] Dynamic light scattering (DLS) measurements showed that these micelles had average hydrodynamic sizes ranging from 130 to 160 nm according to the content of the copolymers.

PEG-HBPAE-A copolymeric micelles were cross-linked by UV irradiation (40 mW/cm^2) in the presence of a highly efficient photoinitiator AIBN (0.05 wt %) in phosphate buffer (PB, pH 7.4, 10 mM). In this study, ^{1}H NMR, FTIR and dynamic light scattering were employed to evaluate the photocross-linking process of the micelles. As shown in Figure 3A, the UV-irradiation resulted in a decrease of micelle sizes. The micelles which were exposed to 60 or 90 min UV-irradiations showed a decrease of diameters for approximately 30 nm, while the micelles exposed to 30-min UV-irradiation demonstrated a smaller size decrease, implying that the time span of 60 min may be suitable for the successful cross-linking of micelles. The resulting CLMs had average particle sizes ranging from 120 to 140 nm and narrow size distribution with polydispersities as low as 0.06−0.14. Both DLS and TEM micrographs pointed to a homogeneous distribution of micelles. TEM revealed that CLM had a clearly spherical morphology with an average size of ca. approximately 100 nm (Figure 1D).

To further evaluate the core-cross-linking, we used a good organic solvent for HBPAE-PEG amphiphilic copolymer to dilute the micelles solution followed by the size determination by DLS (Figure 3B). The size of NCLM was about 160 nm and changed to smaller than 10 nm or even negligible in DLS after addition of a large amount of DMF solvent. The size of CLMs increased from 140 nm to about 360 nm after being diluted by DMF solvent to two times of the original volume, and the narrow polydispersity was observed as low as 0.15, indicating that the nanoparticles were so robust that they kept the core−shell structure even after exposure to highly soluble solvents. However, the CLMs that were exposed to 30 min UV-irradiation showed a prominent increase in size and polydispersity, probably resulting from the partial cross-linking of the core. It may indicate that the 60-min cross-linking process is necessary to produce the favorable core-cross-linking architecture.

Dilution in a large volume of DMEM with the presence of 10% FBS was utilized to investigate the stability of CLMs mimicking i.v. injections. As shown in Figure 3C, when the NCLMs micelle solution was diluted by the DMEM with 10% FBS to the concentration (∼5 μg/mL) lower than the critical micellar concentration (∼10 μg/mL), NCLMs exhibited partially dissociation with the appearance of multiple peaks and elevated PDI values. Whereas the CLMs exhibited almost no change in DLS values in the presence of large amount of DMEM supplement with 10% FBS, indicating the formation of sufficiently stable nanoparticles.

pH sensitivity of CLMs was investigated using the DLS by decreasing the pH value from 7.4 to 4.0. As shown in Figure 3D, the CLMs underwent a size increase from ∼130 nm to ∼240 nm but with a narrow size distribution in presence of an acidic environment which suggested the presence of a stable core−shell structure with a swollen cross-linked core due to the protonation of tertiary amines in HBPAE core. The NCLMs' size varied greatly with a concomitant greatly increasing upon

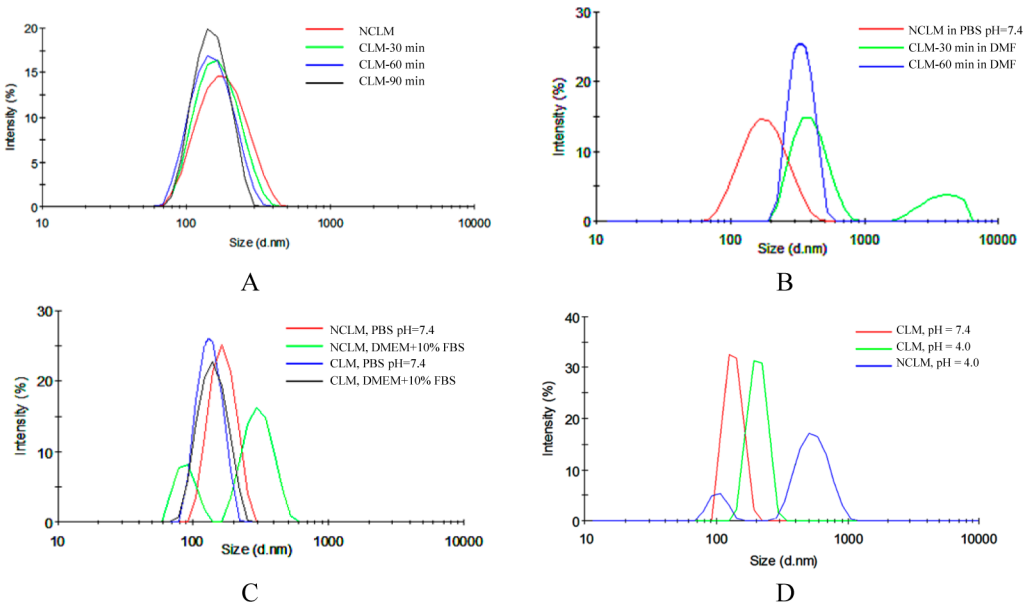

Figure 3. (A) Size distribution of non-cross-linked micelles, cross-linked micelles after UV-irradiation for 30 min, 60 and 90 min; (B) size variation of cross-linked micelles upon exposure to N,N-dimethylformamide; (C) stability of non-cross-linked micelles and cross-linked micelles in the presence of 100-fold dilution by DMEM supplement with 10% FBS; (D) pH sensitivity of cross-linked micelles in pH 7.4, 6.0, and 4.0, respectively. All these results were investigated by DLS with initial concentration of 500 to 800 μg/mL.

decreasing pH value. Both samples had the pH responsiveness resulting from the protonation of tertiary amine groups in the core, however, the CLMs can maintain the core−shell nanoscaled structure attributed by the covalent cross-linking of the core.

The pH-dependent DOX release from the PEG5000-HBPAE CLMs was investigated using dialysis. DOX was loaded into the micelles using the solvent replacement approach followed by the extensive dialysis procedure. The drug loading content of DOX in CLM and NCLM was ∼5 and ∼5.7%, while the drug loading efficiency of DOX in CLMs and NCLMs was ∼56 and ∼60%, respectively. The hyperbranched architecture of the poly(β-aminoester) may contribute to the enhanced drug loading efficiency in comparison to the developed micelles in our previous reported work,[15,17,23] in which the drug loading efficiency can hardly be over 30% in the linear amphiphilic polymeric micelles. At predetermined intervals, 6 mL of immersion solution was taken out from 30 mL fo incubation solution and 6 mL of fresh buffer solution was added to restore the volume to 30 mL. The solutions taken out at different time intervals were characterized by UV−vis spectrometry at 480 nm, which is the characteristic maximum absorbance of DOX in aqueous solution. As shown in Figure 4, there was a slow

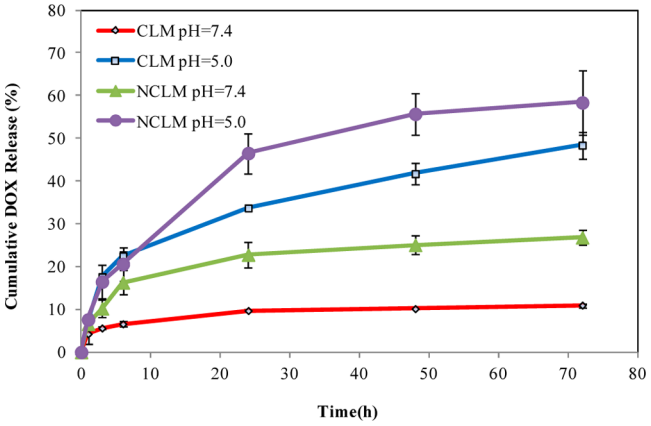

Figure 4. In vitro DOX release curves of DOX-loaded CLMs and NCLMs micelles at 37 °C at pH 7.4 and 5.0, respectively, determined by UV−vis spectrometry.

release of about 10% of the incorporated DOX within 72 h in PBS at pH 7.4. As expected, the rate of DOX release from CLMs in acetate buffer solution at pH 5.0 was much faster, with a 20% release in the first 6 h and up to 50% release in 72 h. As compared to our previous work,[15] these results indicate that the DOX-loaded copolymeric micelles will preserve their core−shell structures at physiological pH, resulting in the small drug molecular diffusion from the core to maintain a slow and sustained release. When the drug-loaded micelles were dispersed in an acidic environment with a pH value lower than 5.0, however, the drug molecules entrapped in the HBPAE core will show enhanced release with swollen core. Particularly, this pH change from 7.4 to 5.0 corresponds to the pH change from extracellular pH to late endosomal pH, probably suggesting that these DOX-loaded CLMs are suitable for intracellular drug delivery. Moreover, the positive-charged core of the micelles and their capacity of disrupting endosomes due to the proton sponge effect may further enhance the approval of the use of these micelles for cytoplasmic drug delivery.

Cell Inhibition of CLMs and NCLMs. MCF-7 and HepG-2 cells were used to measure the cell-inhibition growth rate by utilizing the MTT assay. For this purpose, cells were exposed to different doses of DOX, DOX-loaded micelles and blank micelles. As shown in Figure 5A, blank non-cross-linked

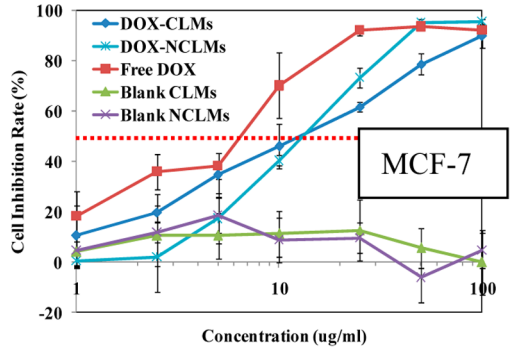

A

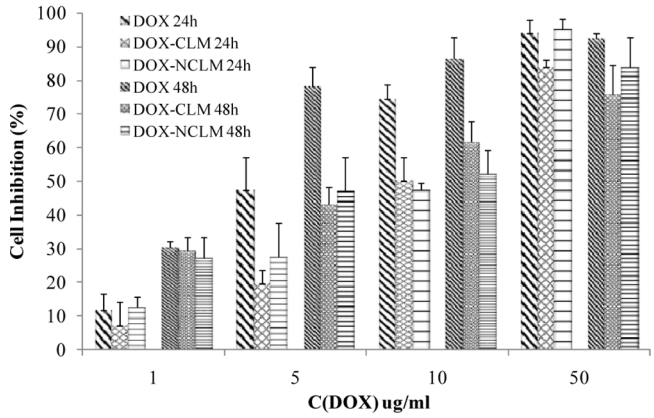

B

Figure 5. (A) MCF-7 and (B) HepG-2 cells inhibition rate as a function of DOX concentrations for free DOX, DOX-loaded NCLMs, DOX-loaded CLMs, and a function of polymer concentrations for blank NCLMs, blank CLMs copolymeric micelles. The point crossing by red dotted line and cell inhibition curve showed half inhibitory concentration (IC50), which is ∼6, ∼12, and ∼12 μg/mL for free DOX, DOX-CLMs, and DOX-NCLMs in MCF-7 cells after 24 h and ∼5, ∼8, and ∼10 μg/mL for free DOX, DOX-CLMs, and DOX-NCLMs in HepG-2 cells after 24 and 48 h, respectively.

micelles and blank CLMs showed minor cytotoxicity in the concentration range of 1−100 μg/mL. This indicated that the cross-linking procedure, especially the addition of initiator, would not increase cytotoxicity of micelles. As expected, the cytotoxicity of DOX increased with increasing dose, whereas the cytotoxicity capacity of the DOX-loaded NCLMs was close to the free doxorubicin in 24 h (Figure 5). The IC50 (the dose having 50% cell inhibition) of nanoparticle-encapsulated DOX was about two times higher than free DOX. It indicated that the cell inhibition efficiency of DOX-loaded CLMs and NCLMS was much lower than that of free DOX, because free DOX can easily diffuse into cytoplasm as a small-molecular drug and exert its function. In contrast, the DOX-loaded CLMS and NCLMs are most likely internalized by endocytosis. To further estimate the in vitro cytotoxicity in different cell line, the 24 and 48 h cell inhibition rate of doxorubicin, we investigated DOX-CLM and DOX-NCLM in HepG2 cells as shown in Figure 5B. In

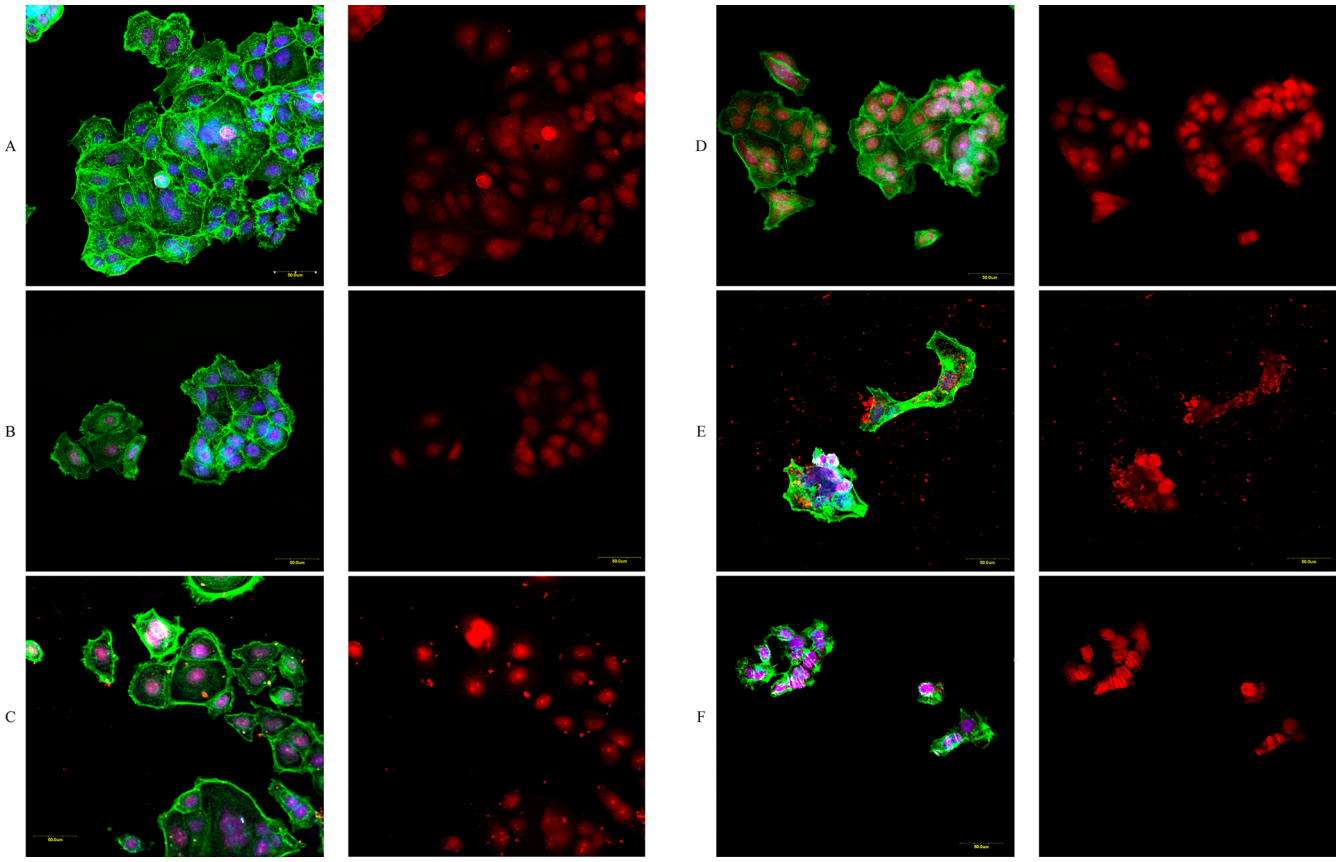

Figure 6. Confocal microscopy images of HepG-2 cells incubated with DOX-CLMs for (A) 15 min, (C) 2 h, and (E) 24 h and with free DOX for (B) 15 min, (D) 2 h and (F) 24 h. For each panel, left images show the overlays of cells with DOX fluorescence, nuclei were stained by Topro-3 and F-actins were stained by BODIPY FL phallacidin, and the images on the right show the DOX fluorescence only. Scale bar = 50 μm.

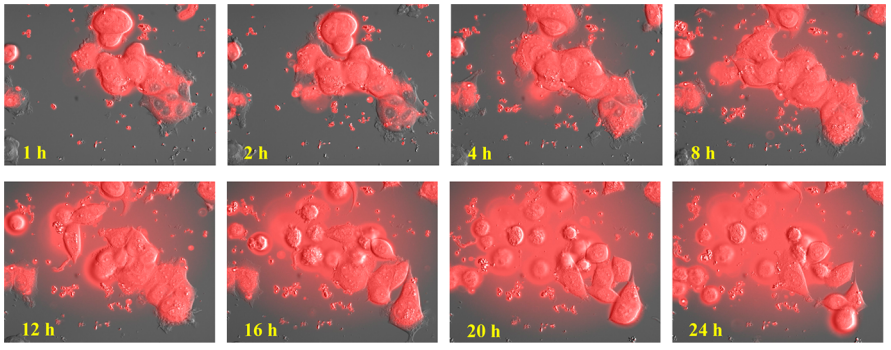

Figure 7. Real-time fluorescence microscopic observation of DOX release in the living MCF-7 cells in 24 h. The cells were visualized with a × 40 objective lens using standard filter sets and a mercury lamp. Sequential images were acquired with a cooled charge-coupled device camera (DP30BW, Olympus) with a certain exposure time every 15 min. Data were analyzed using Image J 1.46 software from NIH.

both time-points, the cell inhibition rate increased by elevating concentration of DOX in agreement with the corresponding ones in MCF-7 cells. When treated by low equivalent dosage of DOX for 48 h (for example 5 ug/mL), IC50 value of either CLMs or NCLMs was more than two times lower than the data of 24 h. Our data show that the synthesized copolymers and copolymeric micelles have very low cytotoxicity and can efficiently deliver DOX to cells with the course of time.

Internalization and Intracellular Drug Distribution. Confocal laser scanning microscopy (CLSM) was employed to examine the cellular uptake and sequential drug distribution of DOX in HepG-2 cells. The cells were seeded in a culture dish with a coverslip at a density of 2 × 10^5 cells/dish (diameter = 3.5 cm) and cultured for 24 h. Subsequently, the cells were exposed to DOX-loaded CLMs micelles and free DOX for further incubation. The nuclei were stained by Topro-3 and changed to a blue color by confocal software. The cytoplasm of the cells was visualized through F-actin stained by BODIPY FL phallacidin.

As shown in Figure 6A, after 15 min incubation, the free DOX was visibly observed and distributed in cell cytoplasm and the nuclei of the HepG-2 cells. Remarkably, after only 15 min of incubation with the DOX-loaded CLMs, DOX fluorescence was also visibly observed in cell cytoplasm and nucleus.

Interestingly, after 2 h exposure to DOX-loaded CLMs, we observed large red dots of DOX fluorescence appeared in the

cytoplasm and accumulate in and around the nuclei. This aggregation of the nanoparticles is ubiquitous during uptake and endsomal escape of the nanoparticles in the cytoplasm demonstrated by a number of studies by other groups, having the similar results of the accumulation of the nanoparticles in the endo/lysosomes and/or then aggregation in the cytoplasm.[40,41] The reason is complicated and unclear currently, which could be probably caused by the degradation of the nanoparticles in the endo/lysosomes and the proteins binding, thus the stability of nanoparticles was damaged and the large aggregates were formed thereby. Stronger red fluorescence appeared overlapping with the nuclei, which indicated DOX was released from the nanoparticles and efficiently intercalated into DNA, forming DNA adducts and inhibiting topoisomerase II.[42] The DOX treatment cells showed the stronger red doxorubicin fluorescence distributed in or around the nuclei. After cell uptake, the efficiently release of doxorubicin was shown by the increased intensity of red doxorubicin fluorescence. After 24 h exposure to free DOX and DOX-loaded CLMs, the nucleus became distinctively swollen and the cytoplasm shrank in comparison to cells that were exposed to these agents for shorter time periods. This observation further supports the effective and efficient delivery of DOX into the cell nuclei by our modified functional cross-linked micelles.

For further real-time investigation of DOX-CLMs into cells, fluorescence, and DIC time lapse images using the Olympus Vivaview FL incubator supply with fluorescence microscopy (LCV110U, Olympus Co., Ltd., Tokyo) were used to visualize the in situ process in MCF-7 cells. As shown in Figure 7, after 1-h stabilization, small amount of drugs was starting to release and distributed throughout the whole cells. Notable, the DOX-CLMs was observed to be dispersed in the DMEM media around the cells. With time lapsed, the red DOX fluorescence became intense, and the cellular morphology changed from stretched to round. After 24-h incubation with DOX-CLMs, most of cells were in round with shrunk cytoplasm and swollen nuclei (a movie file m1 was provided in the supplement data). Images obtained from confocal microscope and real time in situ fluorescence microscope both revealed synthesized DOX-CLMs was a high-efficient intracellular drug delivery system. Although confocal microscopy is still a popular and powerful method to investigate the internalization and colocalization of the nanopartilces in the cells, to better investigate the cell uptake of the nanoparticles in our future work, it may be better to employ fluorescence-lifetime imaging microscopy (FLIM) and phasor analysis to differentiate polymer-mediated drugs from free drugs in the interior of living cells.[43]

CONCLUSIONS

We have demonstrated novel pH-sensitive, biodegradable, and cross-linked micelles for enhanced intracellular doxorubicin delivery. To the best of our knowledge, this is the first time poly(ethylene glycol)-*b*-hyperbranched poly(beta-aminoester)s copolymer have been reported to fabricate the covalently cross-linking micelles for anticancer drug delivery. These cross-linked micelles were observed to be highly stable upon large dilution by fully mimicking the conditions after i.v. injection. MTT assays showed very low cytotoxicity of blank nanoparticles, and similar cell inhibition rate of DOX-loaded NCLMS and CLMs. The fast cell uptake of the DOX entrapped in CLMs was observed by LSCM and real-time in situ fluorescence microscopy. The traditional copolymeric micelles can be upgraded to robust nanogel-like micelles through this simple synthesis routine. The reported remarkable improvement in stability of traditional micelles can enhance antitumor efficacy in vivo, though it may be less significantly important in vitro. Inspired by the promising results in this report, our future work will be focused on the in vivo antitumor assay.

ASSOCIATED CONTENT

Supporting Information

Movie of real-time fluorescence microscopic observation of DOX release in the living MCF-7 cells in 24 h. This material is available free of charge via the Internet at http://pubs.acs.org.

AUTHOR INFORMATION

Corresponding Author

*Fax: 1-204-2757507. E-mail: xing@cc.umanitoba.ca (M.M.X.); Zhong@cc.umanitoba.ca (W.Z.).

Author Contributions

[||]J.C. and J.O. contributed equally to this work.

Notes

The authors declare no competing financial interest.

ACKNOWLEDGMENTS

Our work is supported by the NSERC Discovery Grant and NSERC RTI Grant, Manitoba Institute of Child Health, China 863 Project (Grant 2012AA020504) and National Basic Research Program of China (Grant 2012CB619100). We thank Drs A. Raouf and N. Stephens for the suggestions for the research and manuscript.

REFERENCES

(1) Brannon-Peppas, L.; Blanchette, J. O. *Adv. Drug Delivery Rev.* **2004**, *56*, 1649−1659.
(2) Brigger, I.; Dubernet, C.; Couvreur, P. *Adv. Drug Delivery Rev.* **2002**, *54*, 631−651.
(3) Carter, S. K. *J. Natl. Cancer Inst.* **1975**, *55*, 1265−1274.
(4) Llovet, J. M.; Bruix, J.; Barcelona Clin Liver Canc, G. *Hepatology* **2003**, *37*, 429−442.
(5) Minotti, G.; Menna, P.; Salvatorelli, E.; Cairo, G.; Gianni, L. *Pharmacol. Rev.* **2004**, *56*, 185−229.
(6) Peer, D.; Karp, J. M.; Hong, S.; FaroKhzad, O. C.; Margalit, R.; Langer, R. *Nat. Nanotechnol.* **2007**, *2*, 751−760.
(7) Singal, P. K.; Deally, C. M. R.; Weinberg, L. E. *J. Mol. Cell. Cardiol.* **1987**, *19*, 817−828.
(8) Cui, H. G.; Chen, Z. Y.; Zhong, S.; Wooley, K. L.; Pochan, D. J. *Science* **2007**, *317*, 647−650.
(9) Kataoka, K.; Harada, A.; Nagasaki, Y. *Adv. Drug Delivery Rev.* **2001**, *47*, 113−131.
(10) Duncan, R. *Nat. Rev. Drug Discovery* **2003**, *2*, 347−360.
(11) Kwon, G. S.; Forrest, M. L. *Drug Dev. Res.* **2006**, *67*, 15−22.
(12) Bae, Y.; Fukushima, S.; Harada, A.; Kataoka, K. *Angew. Chem., Int. Ed.* **2003**, *42*, 4640−4643.
(13) Rapoport, N. *Prog. Polym. Sci.* **2007**, *32*, 962−990.
(14) Wang, C.-H.; Wang, C.-H.; Hsiue, G.-H. *J. Controlled Release* **2005**, *108*, 140−149.
(15) Chen, J.; Qiu, X.; Ouyang, J.; Kong, J.; Zhong, W.; Xing, M. M. Q. *Biomacromolecules* **2011**, *12*, 3601−3611.
(16) Lu, C.; Xing, M. M. Q.; Zhong, W. *Nanomed.: Nanotechnol. Biol. Med.* **2011**, *7*, 80−87.
(17) Chen, J.; Zehtabi, F.; Ouyang, J.; Kong, J.; Zhong, W.; Xing, M. M. Q. *J. Mater. Chem.* **2012**.
(18) Liu, M.; Chen, J.; Xue, Y.-N.; Liu, W.-M.; Zhuo, R.-X.; Huang, S.-W. *Bioconjugate Chem.* **2009**, *20*, 2317−2323.
(19) Lynn, D. M.; Langer, R. *J. Am. Chem. Soc.* **2000**, *122*, 10761−10768.

(20) Wu, D. C.; Liu, Y.; Jiang, X.; He, C. B.; Goh, S. H.; Leong, K. W. *Biomacromolecules* **2006**, *7*, 1879−1883.
(21) Zugates, G. T.; Anderson, D. G.; Little, S. R.; Lawhorn, I. E. B.; Langer, R. *J. Am. Chem. Soc.* **2006**, *128*, 12726−12734.
(22) Lee, J.-S.; Green, J. J.; Love, K. T.; Sunshine, J.; Langer, R.; Anderson, D. G. *Nano Lett.* **2009**, *9*, 2402−2406.
(23) Chen, J.; Xing, M. M. Q.; Zhong, W. *Polymer* **2011**, *52*, 933−941.
(24) Shen, Y.; Tang, H.; Zhan, Y.; Van Kirk, E. A.; Murdoch, W. J. *Nanomed.: Nanotechnol., Biol. Med.* **2009**, *5*, 192−201.
(25) Li, Y. L.; Zhu, L.; Liu, Z. Z.; Cheng, R.; Meng, F. H.; Cui, J. H.; Ji, S. J.; Zhong, Z. Y. *Angew. Chem., Int. Ed.* **2009**, *48*, 9914−9918.
(26) Bae, Y. H.; Yin, H. Q. *J. Controlled Release* **2008**, *131*, 2−4.
(27) Cheng, C.; Qi, K.; Germack, D. S.; Khoshdel, E.; Wooley, K. L. *Adv. Mater.* **2007**, *19*, 2830−2835.
(28) Huang, H. Y.; Remsen, E. E.; Wooley, K. L. *Chem. Commun.* **1998**, 1415−1416.
(29) Shuai, X. T.; Merdan, T.; Schaper, A. K.; Xi, F.; Kissel, T. *Bioconjugate Chem.* **2004**, *15*, 441−448.
(30) Talelli, M.; Rijcken, C. J. F.; Oliveira, S.; van der Meel, R.; Henegouwen, P. M. P. v. B. E.; Lammers, T.; van Nostrum, C. F.; Storm, G.; Hennink, W. E. *J. Controlled Release* **2011**, *153*, 93−102.
(31) Wu, D.; Liu, Y.; He, C.; Chung, T.; Goh, S. *Macromolecules* **2004**, *37*, 6763−6770.
(32) Hong, C. Y.; You, Y. Z.; Wu, D. C.; Liu, Y.; Pan, C. Y. *J. Am. Chem. Soc.* **2007**, *129*, 5354−5355.
(33) Boutevin, B.; David, G.; Boyer, C.; Springer-Verlag, B. Telechelic oligomers and macromonomers by radical techniques. In *Oligomers Polymer Composites Molecular Imprinting*; Advances in Polymer Science; Springer: New York, **2007**; Vol. *206*, pp 31−135.
(34) Soeriyadi, A. H.; Li, G.-Z.; Slavin, S.; Jones, M. W.; Amos, C. M.; Becer, C. R.; Whittaker, M. R.; Haddleton, D. M.; Boyer, C.; Davis, T. P. *Polym. Chem.* **2011**, *2*, 815−822.
(35) Boyer, C.; Boutevin, G.; Robin, J. J.; Boutevin, B. *Polymer* **2004**, *45*, 7863−7876.
(36) Boyer, C.; Granville, A.; Davis, T. P.; Bulmus, V. *J. Polym. Sci., Part A: Polym. Chem.* **2009**, *47*, 3773−3794.
(37) Zhang, C. Y.; Yang, Y. Q.; Huang, T. X.; Zhao, B.; Guo, X. D.; Wang, J. F.; Zhang, L. J. *Biomaterials* **2012**, *33*, 6273−83.
(38) Sun, H.; Guo, B.; Li, X.; Cheng, R.; Meng, F.; Liu, H.; Zhong, Z. *Biomacromolecules* **2010**, *11*, 848−854.
(39) Sun, H.; Guo, B.; Cheng, R.; Meng, F.; Liu, H.; Zhong, Z. *Biomaterials* **2009**, *30*, 6358−6366.
(40) Sauer, A. M.; Schlossbauer, A.; Ruthardt, N.; Cauda, V.; Bein, T.; Braeuchle, C. *Nano Lett.* **2010**, *10*, 3684−3691.
(41) Lee, C.-H.; Cheng, S.-H.; Huang, I. P.; Souris, J. S.; Yang, C.-S.; Mou, C.-Y.; Lo, L.-W. *Angew. Chem., Int. Ed.* **2010**, *49*, 8214−8219.
(42) Gewirtz, D. A. *Biochem. Pharmacol.* **1999**, *57*, 727−741.
(43) Duong, H. T. T.; Hughes, F.; Sagnella, S.; Kavallaris, M.; Macmillan, A.; Whan, R.; Hook, J.; Davis, T. P.; Boyer, C. *Mol. Pharm.* **2012**, *9*, 3046−3061.